EAST EUROPEAN JOURNAL OF PHYSICS. 3. 550-563 (2026)
DOI:10.26565/2312-4334-2026-3-50 ISSN 2312-4334

MULTI-FIELD MODULATION OF TUNNELING CURRENT, DIFFERENTIAL RESISTANCE AND NOISE IN n^+–GaAs/AlGaAs TUNNEL DIODES

Mukhammadjon G. Dadamirzaev[1], Munirakhon K. Uktamova[1,2]*, Nosirbek A. Sattarov[3], Sobir Ruziboyev[4], Arofat I. Khudayberdieva[5]

[1]Namangan State Technical University, Namangan, Uzbekistan
[2]University of Business and Science, Tashkent, Uzbekistan
[3]Kimyo International University in Tashkent, Uzbekistan
[4]Tashkent Institute of Irrigation and Agricultural Mechanization Engineers, National Research University, Uzbekistan
[5]Tashkent Institute of Chemical Technology (TICT)
**Corresponding Author e-mail: umk9391@gmail.com*
Received March26, 2026; revised June 22, 2026; in final form July 20, 2026; accepted August 6, 2026

This work presents a theoretical study of differential resistance and noise in tunnel diodes under combined optical, magnetic, and high-frequency electromagnetic fields. The tunneling current is modeled using the Tsu–Esaki approach with WKB approximation, while magnetic field effects are introduced via Landau quantization. Optical excitation leads to quasi-Fermi-level splitting and enhances the tunneling current, thereby modulating and smoothing the negative differential resistance (NDR) region. High-frequency fields further modify the barrier transparency, thereby affecting the device's dynamic behavior. Noise analysis based on shot noise and Fano factor shows that a high signal-to-noise ratio (SNR) can be maintained under external perturbations. A generalized multi-field model for n^+–GaAs/AlGaAs heterostructures is proposed, demonstrating controllable tunneling dynamics, low noise, and stable operation in the sub-THz range. The results indicate strong potential for applications in high-speed optoelectronics and radiation-resistant space electronics.
Keywords: *Tunnel diode; Negative differential resistance; Tsu–Esaki model; WKB approximation; Landau quantization; Shot noise; GaAs/AlGaAs heterostructure; Quasi-Fermi level; High-frequency fields; Optical excitation; Magnetic field effects*

INTRODUCTION

The investigation of quantum tunneling phenomena in semiconductor heterostructures remains an important research area due to its relevance for high-speed and high-frequency electronic devices [1-4]. Tunnel diodes constitute a prominent class of such devices, operating through charge-carrier tunneling across a narrow potential barrier. A tunnel diode is a semiconductor device that operates based on the quantum mechanical tunneling phenomenon [5-7]. This effect was first experimentally observed and theoretically explained by Leo Esaki, who demonstrated negative differential resistance (NDR) in heavily doped p–n junctions [8]. The unique current–voltage (I–V) characteristics of tunnel diodes enable their application in high-speed switching, oscillators, and microwave and terahertz electronic devices. The tunneling process is inherently a quantum mechanical effect in which charge carriers penetrate potential barriers that would be forbidden in classical physics. This phenomenon is typically described using the WKB approximation, which provides an analytical expression for the tunneling probability through a potential barrier [9]. Furthermore, the current in tunnel diodes is commonly modeled using the Tsu–Esaki formalism, which integrates the tunneling probability with the Fermi–Dirac distribution of carriers [1, 10]. The concept of resonant tunneling was later introduced in double-barrier quantum structures by Raphael Tsu and Leo Esaki, leading to the development of resonant tunneling diodes (RTDs) [10, 11]. These devices exhibit extremely fast response times and are capable of operating in the gigahertz and terahertz frequency ranges. Semiconductor heterostructures such as GaAs/AlGaAs and GaN/AlN are widely used due to their favorable electronic properties, including low effective mass and high carrier mobility [12-14]. In the presence of an external magnetic field, the energy spectrum of electrons becomes quantized into discrete levels known as Landau quantization [15, 16]. This quantization significantly influences the density of states and modifies the tunneling probability, resulting in oscillatory behavior of the current. Theoretical foundations of this effect were established by Lev Landau, while further developments were carried out in the context of semiconductor physics [17]. Additionally, optical excitation plays a crucial role in modifying the transport properties of tunnel diodes. Incident light generates nonequilibrium electron–hole pairs, leading to a shift in the quasi-Fermi levels and an increase in the tunneling current [18, 19]. This effect enables optical control of the tunneling process and provides a basis for optoelectronic applications. In recent years, the combined influence of electric, magnetic, optical, and high-frequency electromagnetic fields on tunneling devices has attracted significant research interest. Such multi-field interactions allow for precise control of tunneling dynamics and the negative differential resistance region, which is essential for advanced device engineering. In particular, GaN-based resonant tunneling diodes demonstrate high thermal stability and radiation resistance, making them suitable for harsh environments [20]. However, a comprehensive theoretical model that

Cite as: M.G. Dadamirzaev, M.K. Uktamova, N.A. Sattarov, S. Ruziboyev, A.I. Khudayberdieva, East Eur. J. Phys. 3, 550 (2026), https://doi.org/10.26565/2312-4334-2026-3-50

simultaneously accounts for tunneling, noise, magnetic quantization, and external field effects is still lacking. Understanding the interplay between Landau quantization, quasi-Fermi level splitting, and tunneling probability is essential for the development of next-generation high-speed and low-noise semiconductor devices. In this work, we present a theoretical analysis of the differential resistance and noise characteristics of tunnel diodes under the combined influence of magnetic, optical, and high-frequency fields. The model is based on the Tsu–Esaki formalism, WKB approximation, and Landau quantization, providing a unified description of multi-field effects on quantum tunneling. The obtained results contribute to the development of high-performance nanoelectronic and optoelectronic devices.

METHODS

The tunneling current in a tunnel diode, denoted as $-I$, arising from fully transmitted electrons, is described by the following expression:

$$I(V) = \frac{4\pi e}{h}\int_{-\infty}^{\infty}\left[f_n(E) - f_p(E)\right] T(E,V)\, dE, \tag{1}$$

here, $f_n(E)$and $f_p(E)$ $-$represent the Fermi–Dirac distribution functions in the n- and p-regions, respectively, while $T(E,V)$denotes the tunneling probability, which is typically evaluated using the WKB approximation:

$$T(E,V) \approx \exp\left(-\frac{2}{\hbar}\int_0^d \sqrt{2m(V(x) - E)}\ dx\right), \tag{2}$$

here, $V(x)$ $-$represents the potential energy of the barrier, and $d$denotes the thickness of the p–n junction. The differential resistance is defined as the inverse of the slope of the current–voltage (I–V) characteristic.

$$R_d(V) = \frac{dV}{dI(V)}. \tag{3}$$

Alternatively, it can be expressed as:

$$R_d(V) = \left(\frac{dI}{dV}\right)^{-1}. \tag{4}$$

After calculating the tunneling current within the Tsu–Esaki model, we take its derivative with respect to $-V$.

$$\mathrm{I}_t = \mathrm{A}exp\left(-\frac{4\sqrt{2m}}{3\hbar qF}(qV - E)^{\frac{3}{2}}\right)\int_0^{\mu_n+\mu_p-qV}\sqrt{\varepsilon(\mu_n + \mu_p - \varepsilon - qV)}\cdot\left(\frac{1}{\exp\left(\frac{\varepsilon-\mu_n}{kT}\right)} - \frac{1}{exp\left(\frac{\varepsilon-\mu_n+qV}{kT}\right)+1}\right)d\varepsilon. \tag{5}$$

By adding the diffusion current expression to Eq. (5), the N-shaped current–voltage (I–V) characteristic and the differential resistance of the tunnel diode were theoretically derived within the framework of the WKB approximation under high-frequency electromagnetic excitation. The formation mechanism of the negative differential resistance (NDR) region was explained based on the quantum tunneling process. In this work, the model is extended by taking into account the effect of the magnetic field. Due to the Landau quantization of the electron energy spectrum, the tunneling probability is transformed into a magnetic-field-dependent form. Based on the modified transmission coefficient, the I–V characteristics and differential resistance in the presence of a magnetic field were theoretically obtained and quantitatively compared with experimental data. The obtained results explain the redistribution of current and the shift of the differential resistance region in tunnel diodes under the influence of a magnetic field. In a magnetic field, the transverse motion of electrons becomes quantized, and the energy levels acquire a discrete structure, as demonstrated by Lev Landau

$$E_n = \left(n+\frac{1}{2}\right)\hbar\omega_c, \tag{6}$$

$$\omega_c = \frac{qB}{m}. \tag{7}$$

As a result, the energy spectrum is given by:

$$E = E_z + \left(n+\frac{1}{2}\right)\hbar\omega_c, \tag{8}$$

here, E_z $-$represents the energy component along the tunneling direction. The expressions for the density of states in the presence of a magnetic field are discussed in the article [21].

Due to Landau quantization, the WKB exponential is modified as follows:

$$T_B(E_z) = \exp\left[-\frac{4\sqrt{2m}}{3\hbar qF}\left(qV - E_z - \left(n+\frac{1}{2}\right)\hbar\omega_c\right)^{\frac{3}{2}}\right]. \tag{9}$$

Consequently, the tunneling current takes the following form:

$$I(V,B)=\frac{4\pi q}{\hbar}\sum_{n=0}^{N}\int_{-\infty}^{\infty}T_B(E_z)\,\rho_c(E,B)\,\rho_v(E-qV,B)\,\left[f_n(E)-f_p(E)\right]dE_z. \tag{10}$$

We define in advance:

$$C=\frac{q}{\pi^3\hbar}\left(\frac{2m}{\hbar^2}\right)^3(\hbar\omega_c)^2. \tag{11}$$

Thus, the tunneling current can be written in a compact form as:

$$I_T(V,B)=C\sum_{n=0}^{N}\int_0^{E_{max}}\frac{\left[-\frac{4\sqrt{2m}}{3\hbar qF}\left(qV-E_z-\left(n+\frac{1}{2}\right)\hbar\omega_c\right)^{3/2}\right]}{\sqrt{\left(qV-E_z-\left(n+\frac{1}{2}\right)\hbar\omega_c\right)^{3/2}\left(E_z-\varepsilon_c^{(n)})(E_z-\varepsilon_v^{(n)}-qV\right)}}\cdot\left[f_n(E_z)-f_p(E_z)\right]dE_z, \tag{12}$$

therein:

$$\varepsilon_{c,v}^{(n)}=\varepsilon_{c,v}+\left(n+\frac{1}{2}\right)\hbar\omega_c. \tag{13}$$

This enables a direct comparison of the tunnel diode characteristics $I(V,B)$and $R_d(V,B)$with experimental data. At the same time, under the influence of a magnetic field, the spacing between Landau levels increases, the density of states becomes discrete, the differential resistance region shifts, and the current undergoes oscillatory modulation.

The complete mathematically rigorous form of Eq. (5) under the influence of a magnetic field can be written as follows:

$$I(V,B)=\frac{q}{2\pi^2\hbar l_B^2}\sum_{n=0}^{N}\int_{-\infty}^{\infty}T_B(E_z)[f_n(E_z)-f_p(E_z)]\,dE_z, \tag{14}$$

here,

$$l_B=\sqrt{\frac{\hbar}{qB}}, \tag{15}$$

here, l_B −is the magnetic length, representing the “quantum radius” of the electron’s Landau orbit.

It determines the spatial extent of the wavefunction in the transverse direction and defines the minimal area in phase space corresponding to a single Landau level. In the presence of a magnetic field, electrons undergo classical circular (cyclotron) motion in the transverse plane. From a quantum mechanical perspective, however, the energy levels become discrete—a phenomenon theoretically established by Lev Landau (Landau quantization). Under a magnetic field, the energy space becomes discretized due to Landau quantization. Therefore, the three-dimensional energy integral transforms into a summation over transverse motion and an integral along the tunneling direction. In the weak magnetic field limit, the Landau levels become densely packed, the summation can be replaced by an integral, and the system returns to the classical continuous density of states. Using Eq. (12), the variation of the tunnel diode characteristics under a magnetic field is illustrated in Fig. 1. The theoretical results are compared with the corresponding experimental data reported in the literature [22]. As shown in Fig. 1, with increasing magnetic field induction, the peak value of the resonance in the current–voltage characteristics decreases. This behavior is explained by the increased separation between Landau levels due to stronger quantization and the exponential reduction of the tunneling probability. In the presence of a magnetic field, the transverse motion of electrons becomes quantized, and the number of accessible states decreases, which in turn leads to a reduction in the peak current.

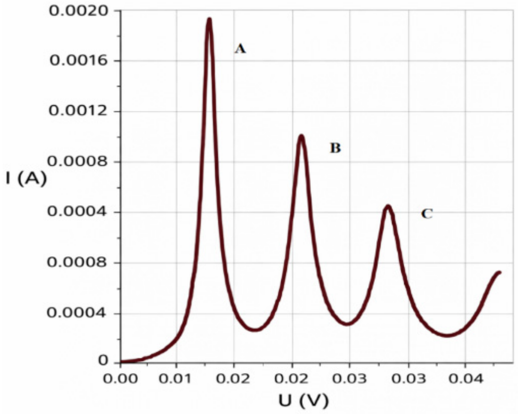

Figure 1. Dependence of the tunneling current on voltage under the influence of a magnetic field

The condition for the differential resistance of a tunnel diode is significantly influenced by the magnetic field, as the spacing between Landau levels increases and the density of states becomes discrete. Numerous experimental studies have investigated the dependence of the peak current on the magnetic field, particularly showing that at low temperatures, the resonance maxima appear sharper and narrower. As the temperature decreases, the Fermi–Dirac distribution function becomes steeper, the energy uncertainty is reduced, and the resonance conditions are satisfied more precisely. As a result, the peak current becomes sharper and its amplitude increases. Conversely, as the temperature increases, the energy distribution broadens, carriers participate over a wider energy range, inter-level transitions become more diffusive, and the resonance peaks broaden while their amplitude decreases.

In this work, the differential characteristic, namely:

$$R_d(V,B) = \left(\frac{\partial I}{\partial V}\right)^{-1}. \tag{16}$$

By substituting the tunneling current expression (12) into Eq. (16), an analytical form of the differential resistance was obtained. Based on the derived results, a three-dimensional distribution of $R_d(V,B)$in phase space was constructed. The dependence of the differential resistance on voltage and magnetic field is illustrated in Figures 2 and 3 in the form of three-dimensional graphs. In addition, the dependence of the differential resistance on voltage and temperature was analyzed while keeping the magnetic field constant. The spatial distribution of $R_d(V,T)$was constructed, revealing the broadening of the resonance region with increasing temperature and changes in the amplitude of the negative differential resistance.

The three-dimensional graphs clearly demonstrate that the differential resistance exhibits sharp variations near the resonance points, its extreme values decrease with increasing magnetic field, and the characteristics become more broadened as the temperature rises.

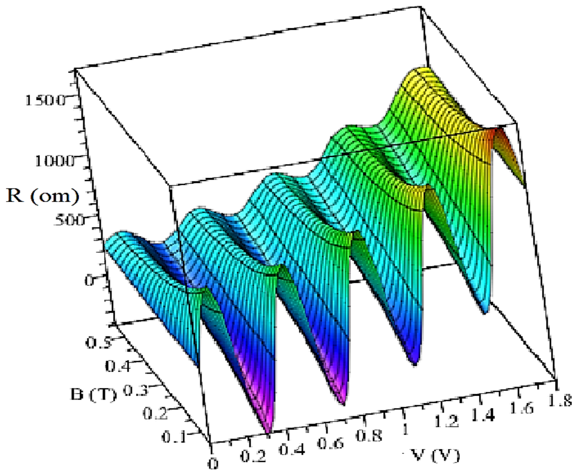

Figure 2. Three-dimensional representation of the differential resistance R_d in phase space, taking into account Landau levels under conditions of a variable magnetic field $B$and constant temperature T

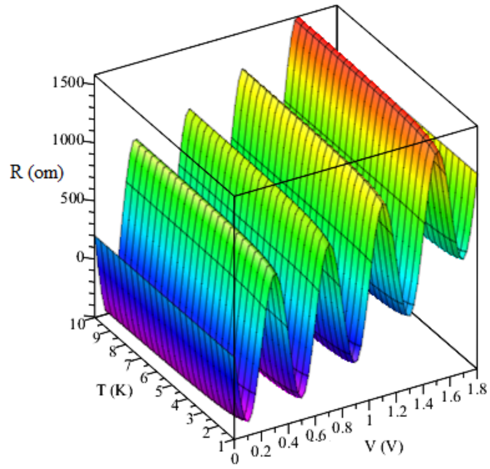

Figure 3. Three-dimensional representation of the differential resistance R_d –as a function of temperature T, considering Landau levels at a constant magnetic field $B = 0.3$ T

As the magnetic field increases, the tunneling transparency of the tunnel diode decreases because electrons are quantized into Landau states. This leads to a reduction in the maximum value of dI/dV, and the differential resistance $R_d(V,B)$increases at the resonance peaks. Consequently, the amplitude of the negative differential resistance (NDR) decreases, which is associated with the reduction of Landau degeneracy and the decrease in the density of quantum states. At low temperatures, the thermal energy of electrons is small; therefore, the tunneling process more accurately reflects the Landau quantized states. Under these conditions, the features of $R_d(V,T)$exhibit sharp and well-defined peaks, and the amplitude of the differential resistance is large. At higher temperatures, while keeping Bconstant, the thermal distribution of electrons broadens, and the Landau levels are thermally smeared. As a result, the peaks of $R_d(V,T)$decrease, and the amplitude of the negative differential resistance is reduced. Thus, the tunneling process is smoothed due to thermal dispersion, and the effects of Landau quantization become less pronounced. The magnetic field and temperature jointly control the tunneling transparency and the amplitude of the differential resistance. Low temperature and weak magnetic field conditions allow Landau quantization to be more clearly observed, whereas higher temperature or stronger magnetic field conditions smooth the resonance peaks and reduce the negative differential resistance. This analysis provides a theoretical and experimental basis for understanding the behavior of tunnel diodes and quantum electronic devices. Since a tunnel diode is based on a heavily doped p–n junction, electrons move within the crystal lattice. Therefore, electrons are not considered free particles in vacuum but rather quantum particles with an effective mass. In the absence of a magnetic field, the electron dispersion relation is given by:

$$E_z = \frac{h^2 k_z^2}{2m^*}, \tag{17}$$

here, m —is the effective mass of the electron. Thus, the model is defined as a three-dimensional degenerate electron gas with an effective mass in the presence of an external uniform magnetic field. Under a magnetic field, when $\mathbf{B} \parallel z$, the electron motion becomes quantized in the transverse plane (Landau quantization), while the motion along the z-direction remains free. The orbital energy is given by:

$$E_n = \hbar\omega_c(n + \tfrac{1}{2}) \ , \omega_c = \frac{qB}{m^*}. \tag{18}$$

The complete energy spectrum is given by:

$$E_{n,k_z} = \hbar\omega_c(n + \tfrac{1}{2}) + \frac{h^2 k_z^2}{2m^*}, . \tag{19}$$

This result indicates that the system effectively transitions into a (2D + 1D) structure. Each Landau level is highly degenerate. The number of states per unit area is given by:

$$\mathrm{g_L} = \frac{qB}{2\pi h}, \tag{20}$$

$\mathrm{g_L} \propto \mathrm{B}$ — the degeneracy is linearly proportional to the magnetic field. The density of states for each Landau level is obtained by considering the energy of each Landau level as:

$$E = E_n + \frac{h^2 k_z^2}{2m^*}. \tag{21}$$

One-dimensional density of states:

$$D_{1D}(E) = \frac{1}{\pi}\sqrt{\frac{m^*}{2\hbar^2}}\frac{1}{\sqrt{E-E_n}}. \tag{22}$$

Total three-dimensional density of states:

$$D(E,B) = \sum_{n=0}^{N_{max}} \frac{\theta(qV-E_n)}{\sqrt{qV-E_n+\varepsilon}} \frac{\theta(\mu_n+\mu_p-qV-E_n)}{\sqrt{\mu_n+\mu_p-qV-E_n+\varepsilon}}. \tag{23}$$

This expression describes the Landau singularities. The tunneling current model is formulated based on the Bardeen approach as follows [21]:

$$I(V,B) = \int_{-\infty}^{\infty} D_n(E,B) D_p(E-qV,B) T(E)\big[f_n(E) - f_p(E)\big]\, dE, \tag{24}$$

here, $D_n(E,B)$denotes the density of states on the electron side, $D_p(E-qV,B)$represents the density of states on the hole side, and $T(E,B)$is the tunneling transparency. The terms $f_n(E)$and $f_p(E)$ —are the Fermi–Dirac distribution functions. A tunnel diode consists of a heavily doped p–n junction, where electrons move within the crystal lattice. Therefore, electrons are not treated as free particles in vacuum but rather as quantum particles with an effective mass.

The transverse component is equivalent to a harmonic oscillator, and the energy levels are given by:

$$E_n = \hbar\omega_c(n + \tfrac{1}{2}), \quad \omega_c = \frac{qB}{m^*}. \tag{25}$$

The total energy available for tunneling is decomposed into transverse and longitudinal (tunneling) components as follows:

$$E = E_n + E_z. \tag{26}$$

The energy along the tunneling direction is given by:

$$E_z = E + \hbar\omega_c(n + \tfrac{1}{2}). \tag{27}$$

As the magnetic field increases, the energy available for tunneling decreases, leading to a reduction in the tunneling transparency $T(E)$. Considering the one-dimensional stationary Schrödinger equation, in quantum mechanics the particle energy is less than the height of the potential barrier:

$$\frac{d^2\psi}{dx^2} + \frac{2m^*}{\hbar^2}\big(E - V(x)\big)\psi = 0. \tag{28}$$

Inside the barrier, $E < \mathrm{q}V$:

$$\frac{d^2\psi}{dx^2} = \frac{2m^*}{\hbar^2}(\mathrm{qV} - E)\psi. \quad (29)$$

The solution has an exponential form:

$$\psi(x) \sim e^{-kx}, \quad (30)$$

here, $k = \frac{\sqrt{2m^*(qV-E)}}{\hbar}$

According to the WKB approximation, the tunneling probability is given by:

$$T(E,B) \approx exp[-2\int_{z_1}^{z_2}\sqrt{\frac{2m^*}{\hbar^2}(qV - E_z)dz}]. \quad (31)$$

For a rectangular barrier:

$$T(E,B) \approx exp[-2d\sqrt{\frac{2m^*}{\hbar^2}\left(qV - E + \hbar\frac{qB}{m^*}\left(n+\frac{1}{2}\right)\right)}. \quad (32)$$

By combining all the physical laws presented above, the tunneling current can be expressed as:

$$I(V,B,h\nu) = \sum_{n=0}^{N_{max}} \frac{\theta(qV - E_n)}{\sqrt{qV - E_n + \varepsilon}} \frac{\theta\left(\mu_n + \mu_p - qV - E_n\right)}{\sqrt{\mu_n + \mu_p - qV - E_n + \varepsilon}} \times$$

$$\times exp\left(-2d\sqrt{\frac{2m^*}{\hbar^2}(qV - E + \hbar\frac{qB}{m^*}(n+\frac{1}{2}))}\right] [\frac{\left(e^{\frac{\mu_n}{kT}}+1\right)\left(e^{-\frac{\mu_p}{kT}}+1\right)}{\left(e^{\frac{\mu_p - qV}{kT}}+1\right)\left(e^{\frac{qV-\mu_n}{kT}}+1\right)}\right). \quad (33)$$

The dependence of the tunnel current on voltage under the combined influence of the UHF and magnetic fields is shown in Fig. 4.

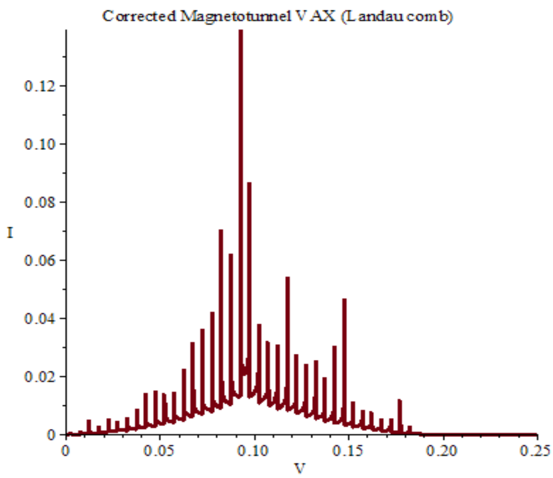

Figure 4. Dependence of the tunnel current on voltage under the influence of ultra-high frequency and a magnetic field

Now, let us derive the expression for the effect of light on a tunnel diode placed in a magnetic field. In this case, since the influence of the magnetic field on the density of states in the tunnel diode is strong, we neglect the filling of the density of states by electrons and holes generated under illumination. Instead, we take into account the broadening (or redistribution) of the density of states caused by the magnetic field.

$$D(E,B) = \sum_{n=0}^{N_{max}} \frac{\theta(qV-E_n)}{\sqrt{qV-E_n+\varepsilon}} \frac{\theta\left(\mu_n+\mu_p-qV-E_n\right)}{\sqrt{\mu_n+\mu_p-qV-E_n+\varepsilon}}. \quad (34)$$

Since we mainly associate tunnel transparency with electron motion, the transparency increases under magnetic influence. The reason for this is that since the density of states changes, it affects the thickness and height of the barrier, and the transparency becomes as follows:

$$T(E,B) \approx exp\left[-2d\sqrt{\frac{2m^*}{\hbar^2}(qV - E + \hbar\frac{qB}{m^*}(n+\frac{1}{2}))}\right]. \quad (35)$$

In these conditions, the only factor that cannot be dominated by the magnetic field is the Fermi–Dirac distribution function. Therefore, charge carriers flow from regions of higher distribution to lower distribution, and this flow gives rise to the distribution function in expression (36).

$$f_n - f_p = \frac{\left(e^{\frac{\mu_n+\Delta\mu}{kT}}+1\right)\left(e^{\frac{\mu_p}{kT}}+1\right)}{\left(e^{\frac{\mu_n-qV}{kT}}+1\right)\left(e^{\frac{qV-\mu_n-\Delta\mu}{kT}}+1\right)}. \tag{36}$$

This behavior mainly reflects quantities such as the effective lifetime of charge carriers generated under illumination and the absorption of light. It is observed that, initially, when light is absorbed in a semiconductor, a generation process occurs, leading to a shift in the chemical potentials. This shift persists until the recombination process begins. During recombination, the effective lifetimes of charge carriers decrease, which in turn leads to a reduction in the chemical potential.

As a result, the current–voltage (I–V) characteristic under the combined influence of light and a magnetic field can be expressed accordingly.

$$I(V,B,h\nu) = \sum_{n=0}^{N_{max}} \frac{\theta(qV-E_n)}{\sqrt{qV-E_n+\varepsilon}} \frac{\theta\left(\mu_n+\mu_p-qV-E_n\right)}{\sqrt{\mu_n+\mu_p-qV-E_n+\varepsilon}} \times$$

$$\times exp\left(-2d\sqrt{\frac{2m^*}{\hbar^2}(qV-E+\hbar\frac{eB}{m^*}(n+\tfrac{1}{2}))} \cdot \frac{\left(e^{\frac{\mu_n+\Delta\mu}{kT}}+1\right)\left(e^{-\frac{\mu_p}{kT}}+1\right)}{\left(e^{\frac{\mu_p-qV}{kT}}+1\right)\left(e^{\frac{qV-\mu_n-\Delta\mu}{kT}}+1\right)}\right). \tag{37}$$

The form of the volt-ampere characteristic of expression (37) above is shown in Fig. 5, which presents the corresponding tunnel current–voltage characteristics under illumination and different magnetic and UHF field conditions.

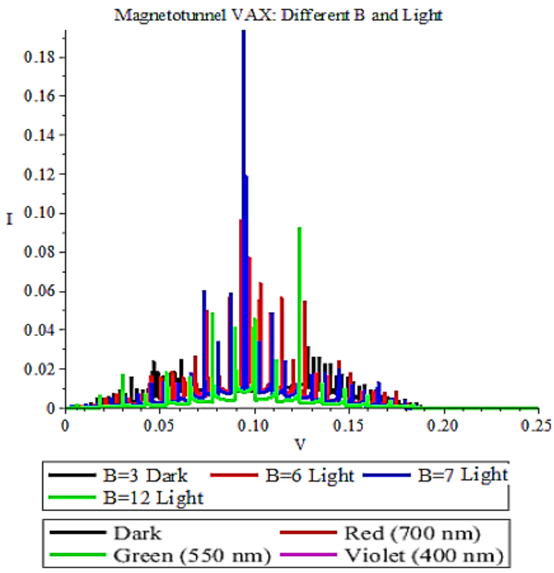

Figure 5. Dependence of the tunnel current on voltage under illumination at different values of magnetic field and ultra-high-frequency field

In this case, the magnetic field values are taken as $B = 3,6,7,12$, while the illumination corresponds to wavelengths of 700 nm, 550 nm, and 400 nm. As can be seen from the graph, the magnetic field quantizes (splits) the density of states into discrete energy levels; as a result, the tunnel current exhibits a comb-like structure.

Now, considering the differential resistance of the tunnel diode under the combined influence of both magnetic field and illumination, we obtain the following expression:

$$R_d(V,B,h\nu) = (\frac{dI}{d\,V})^{-1}. \tag{38}$$

That is, by taking the derivative of the voltage with respect to the current, we obtain the differential resistance. A narrower potential barrier results in a higher transmission coefficient, thereby increasing the tunneling current.

$$(\frac{dI}{d\,V})^{-1} = \sum_n^{\infty} G_n F[-\frac{1}{2(V-E_n)} + \frac{1}{2(\mu_n+\mu_p-qV-E_n)} + \frac{2dm^*}{\hbar^2 k_n}] - \sum_n \frac{G_n}{kT}[f_n - f_p]. \tag{39}$$

If we introduce a tunnel diode into an ultrahigh-frequency field, the charge carriers are simultaneously exposed to the magnetic field and light. This changes the whole theory. In this case, the magnetic field is included in the density of states and transparency, and now we can see in expression (40) that the transparency changes shape due to the presence of an ultrahigh-frequency field.

$$I(V,B,h\nu)=\sum_{n=0}^{N_{max}}\frac{\theta(qV-E_n)}{\sqrt{qV-E_n+\varepsilon}}\frac{\theta(\mu_n+\mu_p-qV-E_n)}{\sqrt{\mu_n+\mu_p-qV-E_n+\varepsilon}}\times$$
$$\times exp\left(-2d\sqrt{\frac{2m^*}{\hbar^2}\left(V_z-qV_{ac}\cos(\omega t)+\hbar\frac{qB}{m^*}\left(n+\frac{1}{2}\right)\right)}\cdot\frac{\left(e^{\frac{\mu_n+\Delta\mu}{kT}}+1\right)\left(e^{-\frac{\mu_p}{kT}}+1\right)}{\left(e^{\frac{\mu_p-qV}{kT}}+1\right)\left(e^{\frac{qV-\mu_n-\Delta\mu}{kT}}+1\right)}\right) \tag{40}$$

We can reduce the above expression for the volt-ampere characteristic of the tunnel current under the influence of an ultra-high frequency (UHF) field, a magnetic field and light to expression (38). We combine it with the expression [23-25], which shows the dependence of the sound signal to noise ratio emitted by the tunnel diode on the tunnel current. Then we can see how the sound signal to noise ratio emitted by the tunnel diode changes in the light energy, UHF and magnetic field in Figures 6-7.

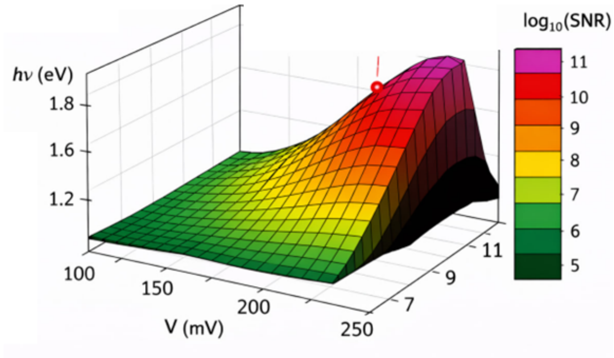

Figure 6. Dependence of the signal-to-noise ratio (SNR) on the differential resistance $R_d$and the photon energy $h\nu$in a tunnel diode

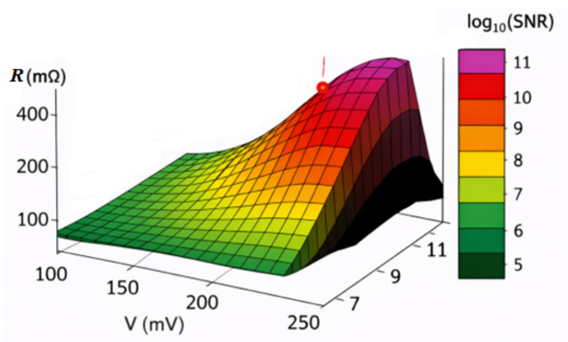

Figure 7. Dependence of the signal-to-noise ratio (SNR) on the photon field (ultra-high-frequency, UHF) and voltage (V)

This graph illustrates the dependence of the signal-to-noise ratio (SNR) on the differential resistance R_d –and the photon energy $h\nu$. A logarithmic scale ($\log_{10}$(SNR)) is used in the graph, so the SNR values start from 5 and reach a maximum point. The colors represent variations in the SNR: from green to red, the SNR increases. The red point indicates the maximum SNR value.

In the graph shown in Figure 7, the colors represent the variation of the SNR, while the red point indicates the maximum SNR value.

If we take into account the drift velocity of electrons in a p–n tunnel junction under an ultra-high-frequency (UHF) field, the following expression can be obtained:

$$\vartheta=\mu E_x. \tag{41}$$

In this expression, μ –denotes the electron mobility, and E_x –represents the electric field strength of the ultra-high-frequency (UHF) field.

Also, the force acting due to the ultra-high-frequency (UHF) field is given by:

$$F=qE_x \tag{42}$$

and the total power influenced by the ultra-high-frequency (UHF) field can be expressed as:

$$P_1=F\vartheta \tag{43}$$

Taking these expressions into account, the power in a p–n tunnel junction under the influence of an ultra-high-frequency (UHF) field can be written as follows:

$$\frac{P_1-P_0}{N}=F\vartheta \tag{44}$$

In this case, N –is the number of electrons, and P_0 –represents the excess fraction of the total power supplied to the diode by the UHF field that corresponds to the sample consumption. If we generalize the above expressions, the power consumed per electron in a p–n tunnel junction under the influence of a UHF field can be written as follows:

$$\frac{P_1-P_0}{N} = q\mu E_x^2 \tag{45}$$

From this expression, the electric field strength E_x −under the influence of the UHF field can be obtained as follows:

$$E_x = \sqrt{\frac{P_1-P_0}{Nq\mu}} \tag{46}$$

The transparency coefficient of the barrier under the influence of the UHF field is expressed as follows:

$$T = \exp\left(-\frac{\alpha E_g^{3/2}}{E+E_x}\right) = \exp\left(-\frac{\alpha E_g^{3/2}}{E+E_x}\right) \tag{47}$$

The dependence of the tunnel current in a tunnel diode on electric and magnetic fields can be summarized as follows:

An increase in the electric field E_x −enhances the probability of electron tunneling, thereby increasing the current. In contrast, a magnetic field Bleads to the formation of Landau quantized energy levels, effectively discretizing the motion of electrons into distinct energy states, which makes the current dependent on the magnetic field. Experimental results confirm that the direct tunneling current in semiconductors decreases under the influence of a strong magnetic field, in agreement with theoretical predictions. Since diffusive tunneling and reverse GaAs diodes were used, and these diodes are characterized by relatively weak electric fields and small effective mass in the p–n junction, a significant reduction in the tunneling current (by 50–65%) was observed. This wide range of variation (at temperatures of 80 K and 300 K) allowed a quantitative comparison between theoretical predictions [26, 27] and experimental data. The results show that the theory developed by Aronov and Pikus provides a good quantitative description of the variation of the tunneling current under a magnetic field. The values of the electric field in the p–n junction, calculated from equation (47), are in good agreement with independently obtained results. The influence of the magnetic field on the excess tunneling current was also observed and studied. The magnitude of this effect is much smaller compared to the direct tunneling region, which can be explained qualitatively based on the concepts developed in [23-25, 28]. If a simple relationship between the electric field and voltage in the p–n junction is assumed, then a satisfactory agreement between theoretical and experimental values of the magnetic field can be obtained in the low-temperature region for excess current. The authors express their gratitude to V. G. Veselago and A. M. Prokhorov for the opportunity to work with the "Solenoid" device, to V. S. Vavilov for collaboration and continuous interest in the work, to V. M. Ivanov and V. M. Karneev for assistance in the experiments, and to G. E. Pikus and A. G. Aronov for valuable discussions of the results. By combining expressions (46) and (47) and substituting the electric field vector Finto equation (40), a more compact expression describing the simultaneous influence of both UHF and magnetic fields on the tunnel current can be obtained. This allows us to visualize the three-dimensional behavior of the current as a function of variations in E_x −and B.

Using equation (40), the variation of the tunnel current under the influence of both the ultra-high-frequency field and the magnetic field is presented in Figure 8.

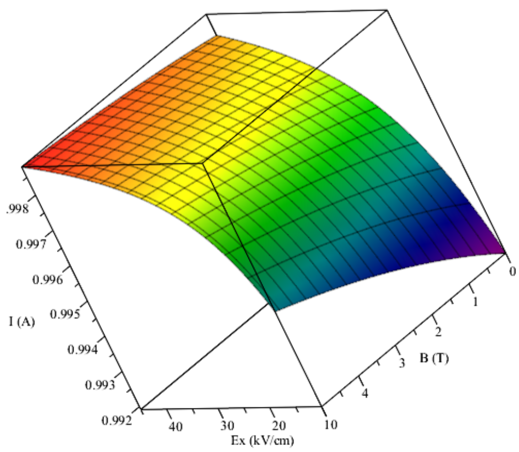

Figure 8. A 3D visualization of the current variation as a function of E_x −and B

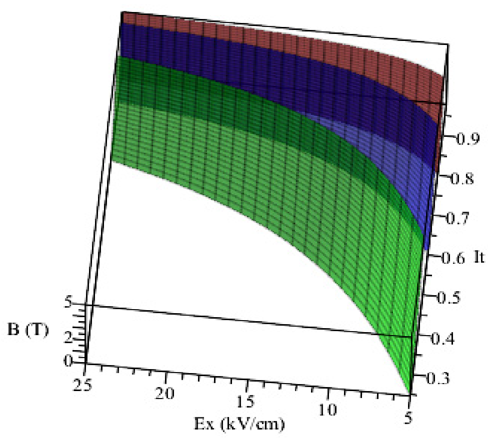

Figure 9. Tunneling current of GaAs-, AlGaAs-, and GaN-based tunnel diodes under the simultaneous influence of ultra-high-frequency and magnetic fields. GaAs—top, AlGaAs—middle, GaN—bottom

Figure 8 illustrates how the current increases from zero or decreases depending on different combinations of E_x −and B. Due to the formation of Landau levels, the step-like behavior of the current with respect to the magnetic field can be observed using the parameters listed in Table 1.

Table 1. Parameters of the semiconductor materials used in the fabrication of the tunnel diode

Parameter	GaAs	InGaAs	GaN
Breakdown field (MV/cm)	~0.4	~0.3	~3.3
Temperature stability	~200°C	~150°C	~600°C
Radiation resistance	Average	Low	Very high
μ_e (sm²/V·s)	~8500	~12000	~1000
(m_e^*/m_0)	0.067	0.12–0.15	0.041
(m_h^*/m_0)	0.45	~0.6	0.45

Using Figure 9 and the parameters given in Table 1, we can observe the three-dimensional spatial distribution of the tunneling current in GaAs-, AlGaAs-, and GaN-based tunnel diodes under the simultaneous influence of ultra-high-frequency and magnetic fields.

Compared to GaAs- and AlGaAs-based tunnel diodes, the tunneling current in GaN-based tunnel diodes is significantly lower. This is mainly due to the wide bandgap of GaN and the larger effective mass of electrons, which reduces the tunneling probability. As a result, GaN diodes exhibit lower maximum tunneling current, making them suitable for applications requiring high voltage and high energy. When light is incident on a semiconductor, electron–hole pairs are generated. This process disturbs the thermodynamic equilibrium of the system and leads to the formation of separate quasi-Fermi levels. As the light intensity increases, the carrier concentration rises, which in turn increases the tunneling current.

Under illumination, the change in electron concentration, $\Delta n(\Phi) -$ is often expressed in a simplified form as

$$\Delta n(\Phi) = \alpha \Phi \tau,$$

where, $\alpha -$is the absorption coefficient, $\Phi -$is the photon flux, and $\tau -$is the carrier lifetime. However, this expression represents only a simplified physical model and is not sufficient for dissertation-level analysis.

In direct bandgap semiconductors such as GaAs, the generation of electron–hole pairs and their recombination mechanisms are more complex. Therefore, a more physically rigorous formulation of $\Delta n(\Phi) -$is required.

Under illumination, both generation and recombination processes occur in a semiconductor. In a steady-state condition, the generation rate equals the recombination rate: $G = R$, where $G -$is the generation rate of electron–hole pairs due to illumination, and $R -$is the recombination rate. For GaAs, taking into account the light spectrum, the generation rate can be expressed as follows:

$$G(\hbar\omega) = \alpha(\hbar\omega)\,\Phi \tag{48}$$

here, $\alpha(\hbar\omega) -$is the optical absorption coefficient, $\Phi -$is the photon flux, and $\hbar\omega -$is the photon energy. For GaAs, the absorption coefficient depends on the photon energy and begins at the bandgap energy $E_g \approx 1.42$ eV (at 300 K).
The recombination process includes three main mechanisms:

- Shockley–Read–Hall (SRH) recombination: occurs at low energy levels, mainly through defects.
- Radiative recombination: electron–hole pairs recombine with the emission of light.
- Auger recombination: occurs at high carrier concentrations and involves energy transfer between carriers.

The total recombination rate can be expressed as follows

$$R = An + Bn^2 + Cn^3 \tag{49}$$

here, A, B, and $C$are the corresponding recombination coefficients, and $n$is the electron concentration. Under steady-state conditions, when generation and recombination are equal, the increase in electron concentration due to illumination for GaAs, $\Delta n(\Phi)$, can be determined as follows:

$$\Delta n(\Phi, \hbar\omega) = \frac{\alpha_0(\hbar\omega - E_g)\,\Phi}{A + Bn_0 + Cn_0^2} \tag{50}$$

this formula:

- $\alpha_0(\hbar\omega - E_g)$— the spectral absorption coefficient of GaAs as a function of photon energy can be expressed as follows:
- n_0—concentration of doped electrons,
- A, B, C — the SRH, radiative, and Auger recombination coefficients, respectively, are:
- Φ — photon flux (photon/sm²·s),
- $E_g \approx 1.42$ eV, 300 K at

This model provides a physical basis for the influence of light intensity and photon energy on the tunneling current, and also allows one to determine the shift of the quasi-Fermi level. Under illumination, the quasi-Fermi level for electrons can be expressed as follows:

$$E_{Fn}(\Phi) = E_F + kT\ln\left(1 + \frac{\Delta n(\Phi,\hbar\omega)}{n_0}\right) \tag{51}$$

Using this, the tunneling current formula under illumination is modulated as follows:

$$I(B, F_\omega, \Phi) = \frac{q^2 B}{2\pi^2\hbar^2}\sum_n \int T(E_n, k_z, F_\omega)\left[f_1\left(E, E_{Fn}(\Phi)\right) - f_2\left(E, E_{Fn}(\Phi) - qV\right)\right] dk_z \tag{52}$$

The resulting dependence of the tunneling current density on magnetic field strength and incident photon energy is presented in Fig. 10. Figure 11 shows the tunneling current as a function of the ultra-high-frequency (UHF) electric field strength and photon energy.

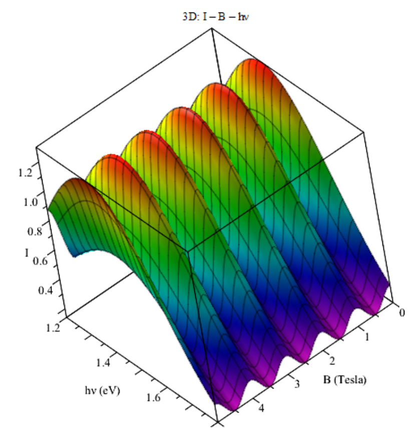

Figure 10. Dependence of the tunneling current density on magnetic field strength and incident photon energy-$h\nu$

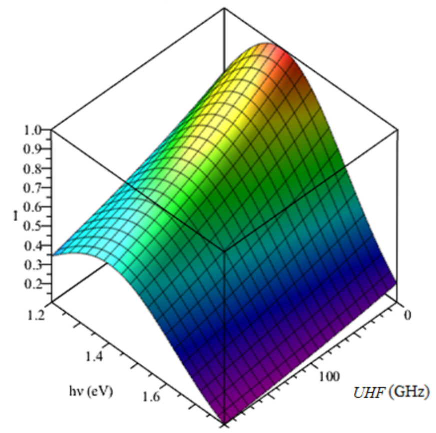

Figure 11. Three-dimensional surface of the tunnel current as a function of high-frequency (UHF) electric field and photon energy (I – UHF – hν)

As the magnetic field increases, the energy spectrum becomes discretized into Landau levels, causing the tunneling probability to exhibit an oscillatory behavior. When the photon energy $h\nu$ −approaches a resonance value, barrier tunneling is enhanced, and the maximum current is observed.

From the graph, it can be seen that as B −increases, quantum oscillations appear in the current, and in the resonance region of $h\nu$ −the tunneling current sharply increases. Magnetic quantization and optical excitation together modulate the current spectrum.

This graph shows the tunneling current as a function of the ultra-high-frequency (UHF) electric field strength and photon energy. The UHF field modulates the internal electric field, thereby changing the tunneling coefficient. As the field strength increases, the tunneling current becomes smoother and decreases (the dynamic barrier widening effect). As the photon energy approaches a resonance value, optical excitation modifies the Fermi–Dirac distribution, and the photocurrent contribution increases. Tunneling is one of the key quantum transport phenomena in semiconductors and was first observed in heavily doped p–n junctions. The tunneling diode effect was theoretically predicted by L. Esaki and later experimentally confirmed [1]. Subsequently, resonant tunneling in double-barrier quantum heterostructures was demonstrated, and the negative differential resistance (NDR) effect was identified. These works laid the foundation for the development of tunnel diodes and resonant tunneling diodes (RTDs). Heterostructures based on III–V semiconductors—such as Gallium Arsenide/Aluminum Gallium Arsenide, Indium Gallium Arsenide, and Gallium Nitride/Aluminum Nitride systems—are among the most promising materials for studying tunneling and quantum transport phenomena. This is mainly due to their band structure, small effective mass, and high electron mobility. GaAs/AlGaAs heterostructures have long been used in resonant tunneling and high-frequency quantum generators. In classical experiments by Chang and collaborators, clear resonant peaks were observed in GaAs/AlGaAs double-barrier structures. Due to the small effective mass of electrons in these structures, the tunneling probability is high, resulting in a strong NDR region and the possibility of terahertz-range generation. InGaAs-based heterostructures exhibit even higher tunneling current intensity due to their smaller effective mass and higher electron mobility. In InGaAs/InP systems, high-frequency generators and detectors operating above 100 GHz have been developed [29]. These structures also exhibit a strong photocurrent effect and operate efficiently in the infrared range. The formation of photocurrent is associated with the trapping and tunneling of photoexcited carriers in quantum wells. GaN/AlN heterostructures, on the other hand, are characterized by a wide bandgap and high electrical strength. These materials are known for their stability under high voltage, high temperature, and strong radiation conditions [9]. In GaN-based structures, strong spontaneous and piezoelectric polarization creates significant internal electric fields, which strongly affect carrier transport in quantum wells. Although the tunneling probability is reduced due to the wide bandgap, GaN/AlN systems are highly promising for space applications and high-radiation environments. Under a magnetic field, Landau quantization of energy levels modulates the tunneling process. In systems with small effective mass such as GaAs and InGaAs, the cyclotron frequency is higher, making the magnetic field effect more pronounced. This leads to quantum oscillations and shifts in the tunneling current maxima [22]. In GaN, although this effect is also present, its modulation amplitude is smaller due to the larger effective mass. Temperature also significantly affects quantum transport. At low temperatures, scattering processes are reduced, and resonant tunneling becomes sharper. At higher temperatures, phonon scattering increases, which broadens the tunneling peaks. GaN/AlN systems can operate stably up to 500–600°C, while GaAs and InGaAs are typically effective in the 150–250 °C range. From the radiation resistance perspective, wide-bandgap GaN/AlN structures have a clear advantage. They are more resistant to cosmic radiation and high-energy particles [30-33]. GaAs-based devices are also widely used in space solar cells [29, 34], but they are more prone to defect formation under radiation. Thus, GaAs/AlGaAs and InGaAs systems are suitable for high-speed quantum and tunneling devices, while GaN/AlN is more promising for high-durability electronics operating under extreme conditions. Their behavior under photocurrent, magnetic fields, high-frequency fields, and across a wide temperature range remains one of the key research directions in tunneling and quantum transport theory.

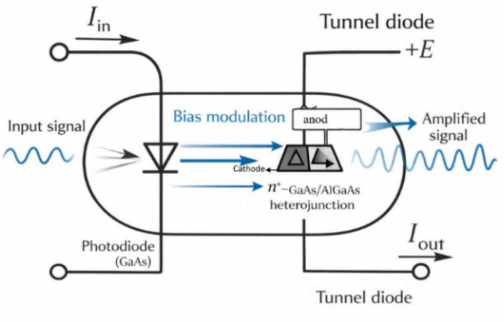

Figure 12. Dependence of tunneling in an n^+-GaAs/AlGaAs heterostructure on light intensity and applied voltage

This study proposes an optically controlled tunneling device based on an n^+–GaAs/AlGaAs tunnel heterostructure. The device operates based on the principle of quasi-Fermi level shift (Δμ) induced by light. The shift in quasi-Fermi levels changes the tunneling window, making the current–voltage (I–V) characteristics sensitive to light intensity. Unlike conventional tunnel diodes, the proposed structure utilizes the band offset of the heterojunction, improving tunneling efficiency and controllability (Figure 12).

Unlike resonant tunneling diodes, the structure does not rely on complex quantum levels, making the fabrication process simpler and more reliable. When light is incident, additional charge carriers are generated in the semiconductor, disturbing equilibrium and causing a separation between quasi-Fermi levels. This additional chemical potential dynamically modulates the tunneling conditions, making the tunneling current dependent not only on voltage but also on light intensity.

Theoretical models qualitatively confirm the optical modulation of the shift in the I–V characteristics and the negative differential resistance (NDR) region. Currently, GaAs/AlGaAs systems are widely used as a key material platform for high-frequency and sub-THz range space electronics. They are distinguished by high electron mobility, short relaxation times, and strong resistance to space radiation, making them highly attractive for aerospace and optoelectronic applications. At the same time, InGaAs systems are suitable for high-speed quantum and tunneling devices, whereas GaN/AlN systems are promising for robust electronics operating under extreme conditions. The behavior of these systems under photocurrent, magnetic fields, high-frequency fields, and wide temperature ranges remains one of the most relevant research directions in the framework of tunneling and quantum transport theory. Thus, optically controlled GaAs/AlGaAs tunnel heterostructures dynamically modulate tunneling through shifts in quasi-Fermi levels, enabling high-frequency operation approaching the sub-THz range. This approach is considered a promising technological solution for space electronics and high-frequency optoelectronic systems. The performance characteristics of tunnel diodes under illumination have been analyzed. It is shown that the superposition of tunnel current and photocurrent leads to a pronounced sensitivity of the I–V characteristics to light intensity, along with a smoothing of the NDR region. Furthermore, analysis based on the Fano factor and shot noise demonstrates that a high signal-to-noise ratio (SNR) is maintained, ensuring stable operation under radiation exposure, temperature variations, and external fields. Within the NASA concept framework, an optically controlled tunnel heterojunction device based on the n^+–GaAs/AlGaAs material system is proposed. In this device, tunneling is dynamically modulated through shifts in the quasi-Fermi levels (Δμ). This approach ensures high-frequency response in the sub-THz range, low noise performance, and radiation hardness, confirming its practical significance for space electronics. The results scientifically substantiate the potential application of resonant tunneling diodes (RTDs) in aerospace systems, high-speed optoelectronic switches, and radiation-resistant sensors.

CONCLUSIONS

This work presents a comprehensive theoretical investigation of tunneling current, differential resistance, and noise characteristics in tunnel diodes under the combined influence of magnetic, optical, and high-frequency electromagnetic fields. Based on the Tsu–Esaki formalism, WKB approximation, and Landau quantization, a unified multi-field model for n^+–GaAs/AlGaAs heterostructures has been developed. The results demonstrate that magnetic fields lead to Landau level formation, causing quantization of the energy spectrum and oscillatory modulation of the tunneling current, accompanied by a reduction in peak current and a shift of the negative differential resistance (NDR) region. Optical excitation induces quasi-Fermi level splitting, enhances carrier concentration, and increases tunneling current while smoothing the NDR characteristics. High-frequency electromagnetic fields dynamically modify the barrier transparency, further influencing the transport properties. It is shown that the interplay of these external fields enables effective control of tunneling dynamics, differential resistance, and device performance. Despite external perturbations, the noise analysis based on shot noise and the Fano factor confirms that a high signal-to-noise ratio (SNR) can be maintained.The proposed model provides a solid theoretical framework for designing low-noise, high-speed tunnel devices operating in the sub-terahertz range. The obtained results indicate strong potential for applications in advanced optoelectronic systems, high-frequency nanoelectronics, and radiation-resistant space technologies.

ORCID

M.G. Dadamirzaev, https://orcid.org/0000-0001-8258-4617; **M.K. Uktamova,** https://orcid.org/0009-0005-7562-2677
N.A. Sattarov, https://orcid.org/0009-0005-0506-0269; **S. Ruziboyev,** https://orcid.org/0009-0005-3176-3515
A.I. Khudayberdieva, https://orcid.org/0009-0005-7163-059X

REFERENCES

[1] S.M. Sze, Y. Li, and K.K. Ng, *Physics of Semiconductor Devices*, 4th Edition, (Wiley, 2021).
[2] B.M. Ali, A.A. Abdulazez, G.P. Priya, S. Ray, A. Pal, R. Sharma, S. Usanov, *et al*., "Modification of graphenylene nanostructure as a promising material for adsorption and sensing of 5-fluorouracil," First-principles investigations. Journal of Molecular Graphics and Modelling, **142**, 109210 (2026). https://doi.org/10.1016/j.jmgm.2025.109210
[3] Z.T. Azamatov, Sh.B. Utamuradova, M.A. Yuldoshev, and N.N. Bazarbaev. "Some properties of semiconductor-ferroelectric structures," East Eur. J. Phys. (2), 187-190. (2023), https://doi.org/10.26565/2312-4334-2023-2-19
[4] M.S. Kukurudziak, V.M. Lipka, and V.V. Ryukhtin, "Silicon p-i-n Mesa-Photodiode Technology, East Eur. J. Phys. (3), 385 (2024). https://doi.org/10.26565/2312-4334-2024-3-47
[5] J.R. Yusupov, M. Ehrhardt, Kh.Sh. Matyokubov, and D.U. Matrasulov, "Driven transparent quantum graphs," Physica Scripta, **100**(7), (2025). https://doi.org/10.1088/1402-4896/ade014
[6] M.A. Yuldoshev, Z.T. Azamatov, A.B. Bakhromov, and M.R. Bekchanova, "Investigation of Morphological and Optical Properties of LiNbO3 and LiNbO3:Fe 0.03 wt.% Crystals," East Eur. J. Phys. (4), 250 (2024). https://doi.org/10.26565/2312-4334-2024-4-25
[7] S. Rakhmanov, K. Matchonov, H. Yusupov, K. Nasriddinov, and D. Matrasulov, "Optical high harmonic generation in Dirac materials," Eur. Phys. J. B, **98**, 35 (2025). https://doi.org/10.1140/epjb/s10051-025-00885-7
[8] L. Esaki, "New Phenomenon in Narrow Germanium p–n Junctions," Phys. Rev. **109**, 603–604 (1958). https://doi.org/10.1103/PhysRev.109.603
[9] E.O. Kane, "Theory of tunneling," J. Appl. Phys. **32**, 83–91 (1961). https://doi.org/10.1063/1.1735965
[10] R.Tsu, and L. Esaki, "Tunneling in a Finite Super lattice," Appl. Phys. Lett. **22**, 562–564 (1973). https://doi.org/10.1063/1.1654509
[11] L.L. Chang, L. Esaki, and R. Tsu, "Resonant tunneling in semiconductor double barriers," Appl. Phys. Lett. **24**, 593–595 (1974). https://doi.org/10.1063/1.1655067
[12] Sh.B. Utamuradova, F.A. Giyasova, K.N. Bakhronov, M.A. Yuldoshev, M.R. Bekchanova, and B. Ismatov. Current Transfer Mechanism in A Thin-Based Heterosystem Based on A^2B^6 Compounds. East Eur. J. Phys. (2025), (3), 325 https://doi.org/10.26565/2312-4334-2025-3-31
[13] U.K. Mishra, P. Parikh, and Y. Wu, "AlGaN/GaN HEMTs-An overview," Proc. IEEE, **90**, 1022 (2002). https://doi.org/10.1109/JPROC.2002.1021567
[14] F.A. Giyasova, A.Z. Rakhmatov, Kh.N. Bakhronov, M.A. Yuldoshev, F.A. Giyasov, A.N. Olimov, and N.A. Sattarov, "Physical Principles of Photocurrent Generation in a Silicon-Based Photodiode Structure with a Schottky Barrier," East Eur. J. Phys. (4), 397 (2025). https://doi.org/10.26565/2312-4334-2025-4-38
[15] L.D. Landau, "Diamagnetism of Metals," Z. Phys. **64**, 629–637 (1930). https://doi.org/10.1007/BF01397213
[16] T. Ando, A.B. Fowler, and F. Stern, "Electronic properties of two-dimensional systems," Rev. Mod. Phys. **54**, 437 (1982). https://doi.org/10.1103/RevModPhys.54.437
[17] A.G. Aronov, and G.E. Pikus, "Magnetic field effects on tunneling," Sov. Phys. Semicond. **10**, 698 (1976). https://doi.org/10.1134/1.1184124
[18] C.H. Henry, "Theory of optical absorption," Phys. Rev. B, **29**, 1619 (1984). https://doi.org/10.1103/PhysRevB.29.1619
[19] L.V. Keldysh, "The effect of a strong electric field on the optical properties of semiconductors," Sov. Phys. JETP, **33**, 994 (1961). https://doi.org/10.1016/0038-1098(65)90052-2
[20] Y. Cao, *et al.,* "Highly repeatable room temperature negative differential resistance from GaN/AlN resonant tunneling diodes," J. Appl. Phys. **120**, 094503 (2016). https://doi.org/10.1063/1.4961442
[21] D.A. Ryndyk, *Theory of Quantum Transport at Nanoscale*, (Springer, 2016). https://doi.org/10.1007/978-3-319-24088-6

[22] E.E. Vdovin, Yu.N. Khanin, O. Makarovsky, Yu.V. Dubrovskii, *et.al.,* "Magnetoanisotropy of electron-correlation-enhanced tunneling through a quantum dot," Physical Review B, 75(11). (2007). https://doi.org/10.1103/physrevb.75.115315
[23] S. Datta, "Quantum Transport: Atom to Transistor," (Cambridge University Press, 2005). https://doi.org/10.1017/CBO9780511805772
[24] M.K. Uktamova, and Sh. Mamadaliev, "Three-dimensional modeling of the relationship between static tunneling and the optical absorption coefficient in tunnel diodes," Results in optics, **22**, 100950 (2026). https://doi.org/10.1016/j.rio.2025.100950
[25] M.G. Dadamirzaev, M.K. Uktamova, Sh. Rakhmanova, and G.A. Ibadullayev, "Simulation of tunnel diode I-V Characteristics with photocurrent and phonon-assisted processes," East Eur. J. Phys. (4), 675-681 (2025). https://periodicals.karazin.ua/eejp/index
[26] M.G. Dadamirzaev, M.K. Uktamova, S.R. Boydedayev, M.A. Yuldoshev, and S.H. Mamadaliev. Theoretical Analysis of Photon-Energy-Controlled Quantum Tunneling Mechanisms Based on the Landauer–Büttiker Formalism. Physics AUC, **35**, 76 (2025). https://share.google/EqKveBzVq9UCc2Ndc
[27] S. Suzuki, *et al.,* "Terahertz oscillation of resonant tunneling diodes," Appl. Phys. Express, 3 064501. (2010). https://doi.org/10.1143/APEX.3.064501
[28] G. Gulyamov, M.G. Dadamirzaev, M.K. Uktamova, and B.Z. Mislidinov, "The effect of a heated electron on the VAX of a tunnel diode," AIP Conference Proceedings 2700, 050007 (2023).
[29] R. Stratton, "Theory of field emission from semiconductors," Phys. Rev. 126 pp. 2002–2014. (1962). https://doi.org/10.1103/PhysRev.126.2002
[30] Sh.I. Nabiyev, K. Bozorov, A. Nasritdinov, R. Ikramov, M. Yuldoshev, N. Sattarov, U. Edilboyev, S. Adilkhan, *et al.,* "Study of the Formation of Radiation Defects in Irradiated Silicon Samples, Doped with Chromium Atoms," East Eur. J. Phys. (1), 228 (2026). https://doi.org/10.26565/2312-4334-2026-1-24
[31] F.A. Giyasova, and M.A. Yuldoshev, "Investigation of temporal characteristics of photosensitive heterostructures based on gallium arsenide and silicon," Chalcogenide Letters, **22**(2), 123–129 (2025). https://doi.org/10.15251/CL.2025.222.123
[32] F.A. Giyasova, K. Bakhronov, M.A. Yuldoshev, M. A., Sapaev, I. B., Ikramov, R. G., Giyasov, F. A., Bekchanova, M. R., *et al.,* "Study of the influence of temperature on the transitions of the CdS/Si/CdTe heterosyste," East Eur. J. Phys. (4), 461 (2025). https://doi.org/10.26565/2312-4334-2025-4-47
[33] M. Asada, and S. Suzuki, "Terahertz Emitter Using Resonant-Tunneling Diode and Applications," Sensors, **21**(4), 1384 (2021). https://doi.org/10.3390/s21041384
[34] M.S. Paizullakhanov, F.A. Giyasova, Kh.N. Bakhronov, M.A. Yuldoshev, A.A. Mamadaliev, F.A. Giyasov, F.T. Akbarova, *et al*., "Investigation of the Processes Involved in the Formation of Pyroxene Materials during Solar Melting in a Large Solar Furnace," Journal of Ovonic Research. **22**(1), (2026). https://doi.org/10.15251/JOR.2026.221.51

БАГАТОПОЛЬОВА МОДУЛЯЦІЯ ТУНЕЛЬНОГО СТРУМУ, ДИФЕРЕНЦІАЛЬНОГО ОПОРУ ТА ШУМУ В ТУНЕЛЬНИХ ДІОДАХ n^+–GaAs/AlGaAs

Мухаммаджон Г. Дадамірзаєв[1], Мунірахон К. Уктамова[1,2], Носірбек А. Саттаров[3], Собір Рузібоєв[4], Арофат І. Худайбердієва[5]
[1]Наманганський державний технічний університет, Наманган, Узбекистан
[2]Університет бізнесу та науки, Узбекистан
[3]Міжнародний університет Кімьо в Ташкенті, Узбекистан
[4]Ташкентський інститут інженерів іригації та механізації сільського господарства, Національний дослідницький університет, Узбекистан
[5]Ташкентський хіміко-технологічний інститут (ТХТІ)

У цій роботі представлено теоретичне дослідження диференціального опору та шуму в тунельних діодах під дією комбінованих оптичних, магнітних та високочастотних електромагнітних полів. Тунельний струм моделюється за допомогою підходу Цу-Есакі з наближенням ВКБ, тоді як ефекти магнітного поля вводяться за допомогою квантування Ландау. Оптичне збудження призводить до квазі-розщеплення рівнів Фермі та посилює тунельний струм, що призводить до модуляції та згладжування області негативного диференціального опору (НДО). Високочастотні поля додатково змінюють прозорість бар'єру, впливаючи на динамічну поведінку пристрою. Аналіз шуму на основі дробового шуму та фактора Фано показує, що високе відношення сигнал/шум (SNR) може підтримуватися при зовнішніх збуреннях. Запропоновано узагальнену багатопольову модель для гетероструктур n^+–GaAs/AlGaAs, яка демонструє керовану динаміку тунелювання, низький рівень шуму та стабільну роботу в субтерагерцовому діапазоні. Результати вказують на значний потенціал для застосування у високошвидкісній оптоелектроніці та радіаційно-стійкій космічній електроніці.

Ключові слова: *тунельний діод; негативний диференціальний опір; модель Цу-Есакі; наближення ВКБ; квантування Ландау; дробовий шум; гетероструктура GaAs/AlGaAs; квазірівень Фермі; високочастотні поля; оптичне збудження; ефекти магнітного поля*